

# 000 001 002 003 004 005 006 007 008 009 010 011 012 013 014 015 016 017 018 019 020 021 022 023 024 025 026 027 028 029 030 031 032 033 034 035 036 037 038 039 040 041 042 043 044 045 046 047 048 049 050 051 052 053 ACHIEVING NOISE ROBUSTNESS BY ADDITIVE NOR- MALIZATION OF LABELS

Anonymous authors

Paper under double-blind review

## ABSTRACT

As machine learning models scale, the demand for large volumes of high-quality training data grows, but acquiring clean datasets is costly and time-consuming due to detailed human annotation and noisy data filtering challenges. To address this, symmetric loss functions were introduced in the context of label noise, enabling models trained on noisy data to perform comparably to those trained on clean data without explicit noise knowledge. Loss functions satisfying a specific symmetry condition exhibit robustness to label noise. Building on this, we propose a novel method to derive noise-robust loss functions using monotonic functions and label normalisation, which involves a simple normalisation of labels that leads to noise robustness when labels are corrupted. Unlike other approaches, this method allows creation of new loss functions by defining application-specific monotonic functions rather than relying on predefined losses. We formally prove their theoretical properties, propose two concrete noise-robust losses, and demonstrate through extensive empirical evaluations on computer vision and natural language processing tasks that our losses outperform standard and existing noise-robust losses. Our evaluations indicate better learning of *decision boundaries*, *faster convergence*, and *improved robustness to noise* using the proposed loss functions.

## 1 INTRODUCTION

The scale of machine learning models has grown dramatically in recent years, fueling remarkable advances across diverse applications such as computer vision, natural language processing, and speech recognition. This rapid growth is primarily due to the advent of transformers (Vaswani et al., 2017), which are trained to predict the next token in a sequence. These transformer models are data-hungry and require vast amounts of corpus data for effective training.

High-quality datasets (Sajith et al., 2024) are essential for training these models effectively, but obtaining such data is often prohibitively expensive and time-consuming. This is mainly because labeling large datasets demands meticulous human annotation and expert domain knowledge, especially for complex tasks. Even in unsupervised learning settings, corpora tend to be noisy due to human errors or corruption during data acquisition from various sources. Moreover, real-world datasets frequently contain noisy or incorrect labels caused by human errors, ambiguity in labeling criteria, or automated labeling processes. Label noise poses a significant challenge because it can cause models to overfit incorrect information, which degrades predictive performance and harms generalization. The problem of label noise is particularly critical in fine-tuning, where models are trained on smaller, domain-specific datasets, making them more sensitive to imperfect labels.

Deep neural networks are particularly susceptible to label noise given their large capacity to memorize training examples, including mislabeled ones. This phenomenon can lead to performance deterioration even when only a fraction of labels are corrupted. Prior work has explored numerous approaches to mitigate the impact of label noise, including data cleaning (Bernhardt et al., 2022), data filtering (Wu et al., 2020), re-weighting samples, and architectural innovations (Jindal et al., 2019; Li et al., 2020; Vashisht et al., 2024; Chen et al., 2020). Among these strategies, the design of noise-robust loss functions has emerged as a theoretically grounded and practically effective direction. Loss functions play a critical role in shaping the learning process by quantifying the discrepancy between predictions and labels, and certain loss functions inherently exhibit robustness to noise by reducing the influence of incorrect labels.

054 A notable theoretical advancement in this domain was introduced by Ghosh et al. (2017), who for-  
 055 malized a symmetry condition that loss functions should satisfy to guarantee robustness to label  
 056 noise. Their framework demonstrated that models trained with such symmetric loss functions on  
 057 noisy data could achieve error rates comparable to models trained on clean datasets, without requir-  
 058 ing explicit knowledge or estimation of the noise characteristics or datasets. This work has lead  
 059 to many follow up investigations. One of these investigations is the concept of normalizing (Ma  
 060 et al., 2020b) loss functions. In this work, any loss function can be divided by sum of losses for  
 061 all class-labels to obtain a noise robust loss function. But, the authors reported that this formula-  
 062 tion lead to underfitting Ma et al. (2020b), and hence had to be added with an active loss (possibly  
 063 non-noise robust) to make the training faster. A similar work Paquin et al. (2024) does the same,  
 064 but not dividing but by subtraction of losses summed over all labels. But, these methods only give  
 065 conditions for obtaining losses from existing losses. This insight has informed the construction of  
 066 novel noise-robust loss functions that offer resilience to common types of label corruption.  
 067

068 Building on this foundation, our work introduces a novel methodology for deriving noise-robust  
 069 loss functions using (only) monotonic functions. We formalize the theoretical properties of these  
 070 transformations, proving that they preserve the symmetry condition necessary for noise robustness.  
 071 Further, we present two specific instantiations of noise-robust losses derived from this framework,  
 072 tailored to balance robustness and optimization tractability. To validate our approach, we con-  
 073 duct extensive empirical experiments spanning computer vision and natural language processing  
 074 benchmarks. Our proposed losses consistently outperform both classical baseline losses and recent  
 075 state-of-the-art noise-robust losses in the literature, demonstrating superior robustness and improved  
 076 model accuracy under various noise regimes.  
 077

078 This study contributes a principled yet practical approach to mitigating label noise effects, enabling  
 079 reliable training of large-scale models in noisy real-world settings. By integrating theoretical rigor  
 080 with empirical validation, our proposed framework advances the understanding and application of  
 081 noise-robust learning in modern machine learning. Our contributions can be summarized as follows:  
 082

- Development of a framework that allows us to design novel application-specific noise-robust loss functions (Section 4)
- Two novel loss functions designed by the above strategy, along with rigorous experimental evaluation. (Section 4.2)
- Our evaluations indicate that the designed loss functions outperform other loss functions in various tasks and show a lesser degradation in performance with an increase in noise level in datasets. Moreover, models trained using our loss functions learn better decision boundaries (Figure 1 and Figure 3) and converge faster compared to other methods (Figure 2).

## 2 PRIOR WORK

090 The quality of a trained machine learning model is primarily influenced by the optimization land-  
 091 scape shaped by the chosen loss function during training. Loss functions guide the model toward  
 092 achieving specific objectives aligned with the task. For example, Intersection over Union (IoU)  
 093 loss Rezatofighi et al. (2019) caters to object detection, cross-entropy loss to classification, and  
 094 Kullback–Leibler (KL) divergence to distribution matching.

095 Among various loss functions, some have been shown to be robust against label noise Ghosh et al.  
 096 (2017), enabling models to learn meaningful patterns despite corrupted labels. However, many  
 097 such noise-robust loss functions are independently designed and are not easily adaptable to existing  
 098 losses.

099 To expand applicability, two important approaches have been proposed to convert existing loss func-  
 100 tions into noise-robust variants: normalization and symmetrization.

101 **Normalization**, (Ma et al., 2020b) in applies a simple normalization step to any loss function to  
 102 theoretically guarantee robustness to noisy labels. Their work proves that by normalizing losses so  
 103 that their values sum to a constant over classes, all losses achieve noise tolerance. However, practical  
 104 use revealed an underfitting problem where normalized robust losses suffered reduced accuracy due  
 105 to diminished learning ability. To mitigate this, they proposed the Active Passive Loss (APL) frame-  
 106 work combining two robust loss functions that mutually improve training effectiveness. Despite  
 107 advancing robustness theory and empirical performance, normalization-based methods still depend  
 108 on existing losses as starting points and can underfit if not carefully combined.

108 **Symmetrization**, studied in (Paquin et al., 2024), constructs noise-robust losses by making them  
 109 symmetric with respect to class labels. Symmetric losses treat all misclassification errors uniformly,  
 110 thereby diminishing the impact of label noise. This approach often involves averaging a loss func-  
 111 tion with its complement or designing inherently symmetric losses. While effective, symmetrization  
 112 techniques require a base loss function with proper structural properties to be converted, thus limit-  
 113 ing their applicability only to certain (permutation invariant) losses.

114 Despite these advances, the need for a pre-existing base loss function to convert into noise-robust  
 115 forms constrains the generality of these methods. Furthermore, applicability can be limited in set-  
 116 tings like reinforcement learning, where the concept of a classical loss function is ambiguous. Re-  
 117inforcement learning focuses on maximizing cumulative rewards rather than minimizing explicit  
 118 losses derived from ground truth labels, making direct application of normalization and symmetriza-  
 119 tion techniques challenging.

### 120 3 PRELIMINARIES

121 Let  $\mathcal{X} \subseteq \mathbb{R}^d$  denote the feature space from which the examples are drawn, and let  $\mathcal{Y} = \{\mathbf{e}_1, \dots, \mathbf{e}_k\}$   
 122 be the set of one-hot encoded class labels, where each  $\mathbf{e}_i \in \{0, 1\}^k$  is a vector with 1 in the  $i$ -th  
 123 position and 0 elsewhere.

124 A classifier learning problem is defined by training data

$$126 \quad S = \{(x_1, \mathbf{y}_{x_1}), \dots, (x_N, \mathbf{y}_{x_N})\} \subseteq (\mathcal{X} \times \mathcal{Y})^N,$$

127 drawn i.i.d. from an unknown distribution  $D$  over  $\mathcal{X} \times \mathcal{Y}$ .

128 We represent a classifier as  $h(x) = \text{pred} \circ p(x)$ , where  $p : \mathcal{X} \rightarrow \mathcal{C}$ ,  $\mathcal{C} \subseteq \mathbb{R}^k$ , and the function  
 129  $\text{pred} : \mathcal{C} \rightarrow \mathcal{Y}$  predicts the class label from  $p(x)$ . For simplicity, we refer to  $p$  itself as the classifier.

130 A loss function is a map  $\ell : \mathcal{C} \times \mathcal{Y} \rightarrow \mathbb{R}^+$ .

131 **Clean risk** is the expected loss evaluated under the true, noise-free distribution  $D$ :

$$134 \quad R_\ell(p) = \mathbb{E}_{(x, \mathbf{y}) \sim D} [\ell(p(x), \mathbf{y}_x)].$$

135 In the presence of label noise, the available data is noisy,

$$137 \quad S_q = \{(x_n, \tilde{\mathbf{y}}_{x_n}), n = 1, \dots, N\},$$

138 where the noisy label  $\tilde{\mathbf{y}}_x$  satisfies

$$140 \quad \tilde{\mathbf{y}}_x = \begin{cases} \mathbf{y}_x, & \text{with probability } 1 - q_x, \\ \mathbf{e}_j \neq \mathbf{y}_x, & \text{with probability } \bar{q}_{xj}, \end{cases}$$

141 with noise rates  $q_x$  and  $\bar{q}_{xj}$  such that  $\sum_{j \neq i} \bar{q}_{xj} = q_x$  for  $\mathbf{y}_x = \mathbf{e}_i$ .

142 The **noisy risk** is the expected loss evaluated on the noisy label distribution  $D_q$ ,

$$144 \quad R_\ell^q(p) = \mathbb{E}_{(x, \tilde{\mathbf{y}}) \sim D_q} [\ell(p(x), \tilde{\mathbf{y}}_x)].$$

145 Let  $p^*$  and  $p_q^*$  be minimizers of the clean risk  $R_\ell(p)$  and noisy risk  $R_\ell^q(p)$ , respectively.

146 Risk minimization under loss  $\ell$  is said to be noise-tolerant if

$$148 \quad \Pr_D [\text{pred} \circ p^*(x) = \mathbf{y}_x] = \Pr_D [\text{pred} \circ p_q^*(x) = \mathbf{y}_x].$$

### 150 4 PROPOSED METHOD: ADDITIVE NORMALIZATION OF LABELS

151 We formulate loss functions for a  $k$ -class classification problem. Consider the loss function as

$$156 \quad \ell(\mathbf{y}, (\mathbf{p})) = -\langle \mathbf{y}, \mathbf{f}(\mathbf{p}) \rangle.$$

158 Here,  $\mathbf{y} \in \{0, 1\}^k$  is the label represented as a one-hot vector, and

$$159 \quad \mathbf{f}(\mathbf{p}) = (f_1(p_1), \dots, f_k(p_k)),$$

160 where the functions  $f_1, \dots, f_k : \mathbb{R} \rightarrow \mathbb{R}$  are strictly increasing monotonic functions, and  $p_1, \dots, p_k$   
 161 are model prediction probabilities for each label.

162 It can be easily seen that minimizing this loss recovers the true label for any choice of monotonic  $f_i$ ,  
 163 i.e.,

$$164 \arg \min_{\mathbf{p}} \ell(\mathbf{e}_i, \mathbf{p}) \implies p_i = 1$$

166 for any one-hot vector  $\mathbf{e}_i, i \in \{1, \dots, k\}$ .

167 Examples of losses in this category include cross-entropy loss with  $f_i(p) = \log(p)$  and linear loss  
 168 with  $f_i(p) = p$ .

169 Within this structure of losses, we now describe the additive normalization of labels.

#### 171 4.1 ADDITIVE NORMALIZATION OF LABELS

172 To illustrate the effect of label normalization in the presence of label noise, we begin with a simple  
 173 binary classification setting. Unlike standard one-hot labels, here the label vectors are defined as  
 174 transformed one-hot vectors:

$$175 \bar{\mathbf{y}} \in \{(-1, 1), (1, -1)\}.$$

176 Noisy labels  $\tilde{\mathbf{y}}$  are generated by flipping the true label  $\bar{\mathbf{y}}$  with probability  $q$ , uniformly, i.e.,

$$177 \tilde{\mathbf{y}} = \begin{cases} \bar{\mathbf{y}} & \text{with probability } 1 - q, \\ -\bar{\mathbf{y}} & \text{with probability } q. \end{cases}$$

180 We define the loss function for prediction  $\mathbf{f}(\mathbf{p}) = [f_1(\mathbf{p}), \dots, f_k(\mathbf{p})]$  as the negative inner product  
 181 of the noisy label and the prediction:

$$183 \ell(\tilde{\mathbf{y}}, \mathbf{f}(\mathbf{p})) = -\langle \tilde{\mathbf{y}}, \mathbf{f}(\mathbf{p}) \rangle.$$

184 Taking the expectation of this loss over the noisy labels conditioned on the true label  $\bar{\mathbf{y}}$  yields:

$$186 \mathbb{E}_{\tilde{\mathbf{y}}|\bar{\mathbf{y}}} [\ell(\tilde{\mathbf{y}}, \mathbf{f}(\mathbf{p}))] = (1 - q)(-\langle \bar{\mathbf{y}}, \mathbf{f}(\mathbf{p}) \rangle) + q(-\langle -\bar{\mathbf{y}}, \mathbf{f}(\mathbf{p}) \rangle) \\ 187 = (1 - q)(-\langle \bar{\mathbf{y}}, \mathbf{f}(\mathbf{p}) \rangle) + q\langle \bar{\mathbf{y}}, \mathbf{f}(\mathbf{p}) \rangle \\ 188 = (1 - 2q) \cdot (-\langle \bar{\mathbf{y}}, \mathbf{f}(\mathbf{p}) \rangle).$$

190 This result implies that

$$191 \mathbb{E}_{\mathcal{X} \times \mathcal{Y}} \ell(\bar{\mathbf{y}}, \mathbf{p}) = (1 - 2q) \mathbb{E}_{\mathcal{X} \times \mathcal{Y}} \ell(\bar{\mathbf{y}}, \mathbf{p}).$$

192 Hence, when  $q < \frac{1}{2}$ , the minimizer of the expected *clean* risk coincides with the minimizer of the  
 193 expected *noisy* risk, demonstrating robustness to noise under this condition.

194 This analysis generalizes to multi-class classification with  $k$  classes as follows. Given a one-hot  
 195 encoded label  $\mathbf{y} \in \{0, 1\}^k$  and a noisy label  $\tilde{\mathbf{y}}$  flipped uniformly with probability  $q$ , define the  
 196 modified vector label vector by applying **additive normalization of labels** as:

$$197 \bar{\mathbf{y}} = \frac{1}{k-1} (k\mathbf{y} - \mathbf{1}), \tag{1}$$

200 where  $\mathbf{1}$  is the all-ones vector in  $\mathbb{R}^k$ .

201 The conditional expectation of the noisy transformed label is:

$$202 \mathbb{E}[\tilde{\mathbf{y}} | \mathbf{y}] = \frac{1}{k-1} (k \mathbb{E}[\tilde{\mathbf{y}} | \mathbf{y}] - \mathbf{1}) \\ 203 = \frac{1}{k-1} \left( k \left( (1-q)\mathbf{y} + \frac{q}{k-1}(\mathbf{1} - \mathbf{y}) \right) - \mathbf{1} \right) \\ 204 = \frac{1}{k-1} \left( \left( k - \frac{k^2q}{k-1} \right) \mathbf{y} + \left( \frac{kq - k + 1}{k-1} \right) \mathbf{1} \right) \\ 205 = \left( 1 - \frac{kq}{k-1} \right) \bar{\mathbf{y}}.$$

212 Accordingly, the expected loss with prediction  $\mathbf{f}(\mathbf{p})$  is:

$$213 -\langle \mathbb{E}[\tilde{\mathbf{y}} | \mathbf{y}], \mathbf{f}(\mathbf{p}) \rangle = -\left( 1 - \frac{kq}{k-1} \right) \langle \bar{\mathbf{y}}, \mathbf{f}(\mathbf{p}) \rangle. \tag{2}$$

215 This results in the following theorem:

216 **Theorem 1.** Consider any loss function defined as  
 217

$$218 \quad \ell(\mathbf{y}, \mathbf{p}) := -\langle \bar{\mathbf{y}}, \mathbf{f}(\mathbf{p}) \rangle,$$

219 where  $\bar{\mathbf{y}}$  is defined by the additive normalization in equation 1. Then, the minimizer of the clean risk  
 220 is the same as the minimizer of the noisy risk provided the noise probability satisfies  
 221

$$222 \quad q < \frac{k-1}{k}.$$

225 *Proof.* The proof directly follows from eq. (2)  $\square$   
 226

227 **Some remarks on the above theorem 1.** It can be verified that even with the proposed normalization  
 228 minimization of the losses recovers the true labels due to the monotonic increasing property  
 229 of  $f_i$ s. 2. The label normalization leads to the condition that  $\sum_{\mathbf{y} \in \mathcal{Y}} \ell(\mathbf{y}, \mathbf{p}) = 0$ . Therefore by  
 230 the robustness theorem by Ghosh et al. (2017) the proposed normalization is also robust to *class*  
 231 *conditional noise and instance dependent noise*.

#### 232 4.2 LOSS FUNCTIONS DESIGNED BY THE ABOVE NORMALIZATION

233 **Noise Robust Focal Loss (NRFL):** NRFL is a noise-robust adaptation of the popular focal loss. The  
 234 focal loss is defined as  $L_{\text{FL}}(p) = -(1-p)^\gamma \log p$ , which down-weights well-classified examples to  
 235 focus training on hard samples. Incorporating focal loss into our noise robustness framework, the  
 236 noise-robust version (NRFL) is computed as

$$237 \quad \ell(p, e_t) = -L_{\text{FL}}(p_t) + \sum_{\substack{j=1 \\ j \neq t}}^k \frac{1}{k-1} L_{\text{FL}}(p_j),$$

241 where  $p_t$  is the predicted probability for the true class  $t$ , and the summation averages over the  
 242 probabilities of other classes. This formulation balances loss contributions to improve robustness  
 243 against label noise.

244 **Weighted Robust Log Loss (WRLL):** WRLL is derived from Robust Log Loss designed to solved  
 245 the class imbalance problem. This is done by computing the weights  $\alpha$  value for each class as  
 246  $\alpha_i = \frac{1}{\text{frequency of } i^{\text{th}} \text{ token}}$ . According to our framework, the label-specific loss is computed as  
 247  $f_i(p) = \log(\alpha_i + p)$ . Thus, WRLL is computed as

$$248 \quad L(p, e_t) = -f_i(p_t) + \sum_{j=1, j \neq t}^k \frac{1}{k-1} f_i(p_j)$$

251 The main advantage of WRLL over RLL is that the loss computed for the  $i^{\text{th}}$  label is dependent on  
 252 its frequency in the training data.

#### 253 **Advantages of Label Normalization over Loss Normalization**

- 254 • Label normalization can be applied in scenarios such as reinforcement learning, where a  
 255 well-defined loss function may not exist but labels or target signals remain well-defined  
 256 and meaningful.
- 257 • It is computationally simpler to implement, as it involves straightforward transformations  
 258 on labels, whereas loss normalization often requires additional complex computations dur-  
 259 ing model training.

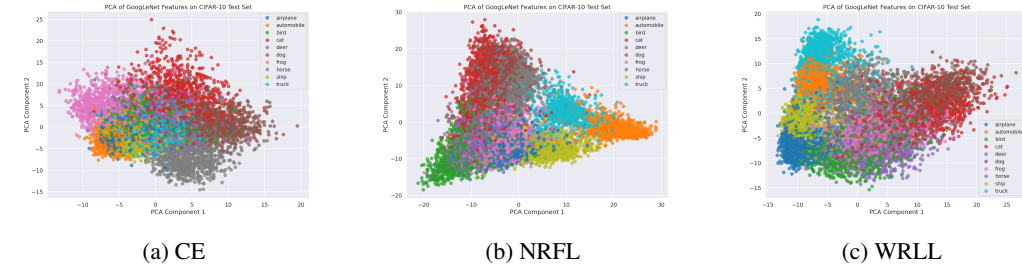
## 260 5 EXPERIMENTS

261 This section presents experimental results comparing NRFL and WRLL against standard and noise-  
 262 robust loss functions including Cross Entropy (CE), Mean Absolute Error (MAE), RLL, and Normalised  
 263 Focal Loss (NFL) (Ma et al., 2020a). Extensive experimentation has been conducted across  
 264 two major domains: computer vision and natural language processing. For datasets without a pre-  
 265 defined validation set, we partition the original training set into training and validation subsets using  
 266 an 80:20 split. Details of the experimental setup, including hyperparameters and the methodology  
 267 for introducing noise into different datasets, are provided in Appendix A.

268 In all result tables, we highlight the top two performing methods: the best-performing method is  
 269 shown in **bold**, while the second-best is indicated with a **grey highlight**. Next, we present our  
 evaluation on object classification tasks.

270 5.1 EVALUATION ON OBJECT CLASSIFICATION TASKS  
271

272 To assess the robustness of NRFL and WRLL in the presence of label noise, we train separate models  
273 using these loss functions, along with the baselines described in Section 4, on three benchmark  
274 datasets: Modified National Institute of Standards and Technology (MNIST) (LeCun et al., 1998),  
275 Fashion-MNIST (Xiao et al., 2017), and Canadian Institute for Advanced Research-10 (CIFAR-  
276 10) (Krizhevsky, 2009). Each dataset consists of approximately 60k training samples, 10k testing  
277 samples, and 10 classes. For every dataset, we introduce label noise at two levels (30% and 60%),  
278 and create two instances of each noise level. We report both the mean accuracy and its standard  
279 deviation across 2 instances of each noise variant.



280  
281 Figure 1: Comparison of decision boundaries for GoogleNet trained on 50% noisy CIFAR-10 using:  
282 (a) CE (b) NRFL (c) WRLL  
283  
284

285 In our initial set of experiments (Table 1), we trained GoogleNet for 15 epochs on each of the three  
286 datasets under varying noise conditions. Each experiment was repeated twice on each noise level  
287 and the mean and standard deviation of the accuracy are reported in Table 1. We observe that models  
288 trained with noise-robust loss functions demonstrate greater resilience to noise, maintaining similar  
289 or only slightly degraded performance with an increase in noise level. This trend holds across all  
290 methods in Table 1, with the exception of the standard cross-entropy loss, which is not a noise-robust  
291 training technique. Among the compared loss functions, NRFL and WRLL consistently achieve  
292 better performance in most evaluation scenarios.  
293

Loss Type	MNIST			CIFAR10			Fashion MNIST		
	0%	30%	60%	0%	30%	60%	0%	30%	60%
CE	99.47	98.71	97.76	82.67	76.1	73.41	92.63	90.97	86.47
MAE	99.33	98.74	<b>99.26</b>	81.44	79.28	79.11	90.26	<b>92.22</b>	<b>92.13</b>
NFL	99.4	95.32	93.55	80.49	74.56	68.83	92.86	90.61	86.84
RLL	99.34	<b>99.11</b>	<b>99.26</b>	82.35	78.6	73.93	93.09	89.83	91.79
GCE	98.27	98.42	90.14	76.82	66.99	46.44	90.43	87.42	84.79
APL	99.35	98.23	98.18	71.19	78.27	50.53	87.05	89.54	88.84
WRLL*	<b>99.59</b>	98.78	99.12	79.93	<b>79.49</b>	77.93	<b>93.47</b>	91.62	90.12
NRFL*	99.38	<b>99.21</b>	98.82	<b>82.71</b>	78.83	<b>79.66</b>	93.28	89.46	81.87

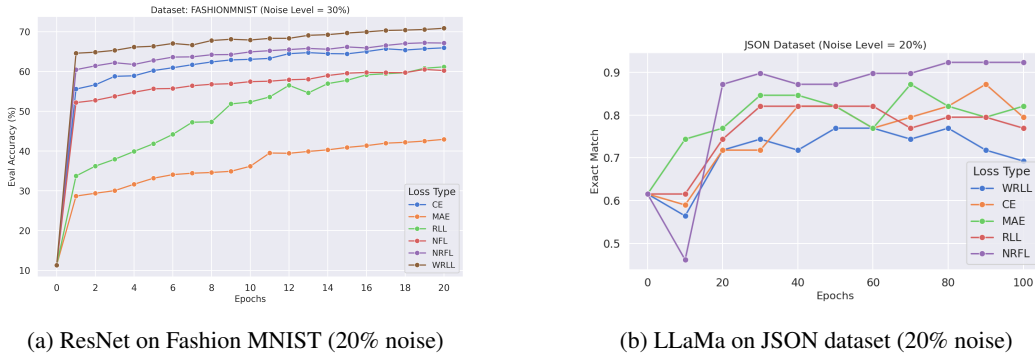
318 Table 1: Accuracy of GoogleNet trained on various datasets after 15 epochs  
319

320 To determine the reason for the superior performance of NRFL and WRLL, we analysed the  
321 representations learned by GoogleNet (Szegedy et al., 2015) trained on the CIFAR-10 dataset with 60%  
322 label noise, using CE, NRFL, and WRLL loss functions. Feature representations were extracted  
323 from the trained models on the CIFAR-10 test set, and Principal Component Analysis (PCA) was  
324 applied to project them into two dimensions for visualisation (Figure 1). As shown in Figure 1,

models trained with NRFL and WRLL exhibit clearer class separation compared to CE, forming distinct clusters aligned with CIFAR-10 labels. Beyond qualitative inspection, we quantified clustering quality using the Silhouette Score (Rousseeuw, 1987), obtaining values of 0.046 for CE, 0.18 for NRFL, and 0.1539 for WRLL. These results confirm that NRFL and WRLL yield more well-defined decision boundaries than CE even under severe label noise (60%).

Loss Type	MNIST			CIFAR10			Fashion MNIST		
	0%	30%	60%	0%	30%	60%	0%	30%	60%
CE	73.5	61.35	58.49	34.43	28.83	27.39	73.3	67.2	65.54
MAE	53.81	56	35.23	23.68	22.78	15.8	69.37	61.41	53.39
RLL	75.51	72.05	62.9	33.55	31.6	25.83	74.45	71.95	68.1
NFL	65.27	46.37	42.56	32.03	28.84	23.05	72.2	68.56	64.03
NRFL	80.29	70.98	67.03	34.61	31.85	26.61	75.63	68.83	67.03
WRLL	<b>81.03</b>	<b>78.46</b>	<b>68.92</b>	<b>37.57</b>	<b>33</b>	<b>32.4</b>	<b>79.59</b>	<b>72.79</b>	<b>70.73</b>

Table 2: Accuracy of Early Stopping of ResNet trained on various datasets after 30 epochs  
In our second set of experiments, we employed a larger architecture than GoogleNet, namely ResNet18 He et al. (2016), which consists of around 11.7 million parameters. Following a methodology similar to that of GoogleNet, ResNet18 was trained for 30 epochs with early stopping. The hyperparameter  $\gamma$  for NRFL was fixed at 0.01. Owing to the higher computational cost of training ResNet, only a single instance per noise level was used. As reported in Table 2, models trained with WRLL and NRFL consistently outperform other methods across most scenarios. This superior performance can again be attributed to the more robust decision boundaries learned with these losses, as reflected in Figure 1 and the corresponding Silhouette scores. [We have also conducted similar experiments for ResNet-18 on the CIFAR-100 \(Krizhevsky, 2009\) dataset, which are presented in Appendix B.2.](#) In addition to improved decision boundaries, models trained with the proposed



(a) ResNet on Fashion MNIST (20% noise)

(b) LLaMa on JSON dataset (20% noise)

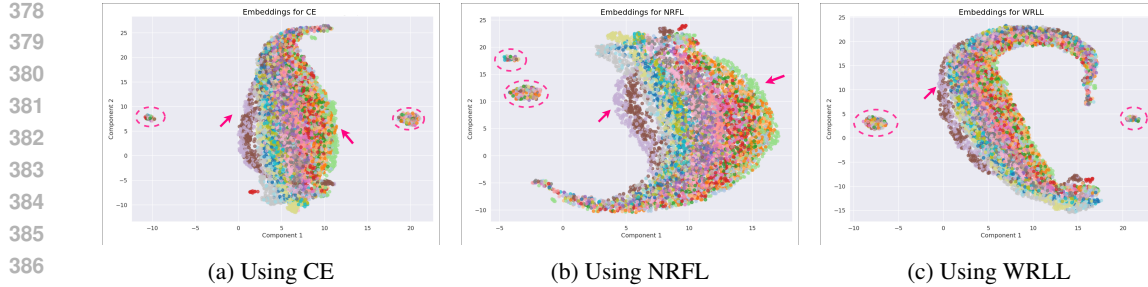
Figure 2: Convergence trajectory of different models trained using different loss functions

NRFL and WRLL loss functions demonstrate faster convergence compared to alternative methods. This behaviour is illustrated in Figure 2a, which shows that across training epochs, models trained with WRLL and NRFL consistently outperform other loss functions. These results suggest that models trained using NRFL and WRLL learn decision boundaries much faster than other methods. Following this analysis, we extend our evaluation to natural language processing (NLP) tasks to assess the generalizability of our findings.

## 5.2 EVALUATION ON NLP TASKS

We evaluate the proposed methods on five natural language processing (NLP) tasks arranged in increasing order of difficulty. Experiments are conducted with two distinct models: meta-llama/Llama-3.2-1B-Instruct (Meta AI, 2024) and Qwen/Qwen2.5-0.5B-Instruct (Team, 2025). In the subsequent text, we refer to these models as LLaMA and Qwen, respectively.

**NLP-based classification task (News20 Dataset) :** Extending on our computer vision experiments, we next explore whether similar trends hold for NLP classification tasks with Large Language Models (LLMs). To do so, LLaMA was trained on the News20 dataset (Lang, 1995) with 20% label



388 Figure 3: Decision boundaries learnt by LLaMA on 20% noisy News20 dataset

Loss Type	Accuracy	Calsinski Score
CE	45.46	38.67
NRFL	<b>63.95</b>	<b>39.05</b>
WRLL	56.72	20.91

395 Table 3: LLaMa trained on 20% noisy News20 dataset

398 noise. Table 3 reports the metrics for models trained with CE, NRFL, and WRLL. Among these,  
399 NRFL attains the highest accuracy and the best Calinski score (Caliński & Harabasz, 1974), indicating  
400 that it learns the best representations among all three. Figure 3 presents a visual representation  
401 of the embeddings learned by LLaMA. This is consistent with Table 3 as models trained with NRFL  
402 outperform those trained with CE and WRLL. As shown in the figure, the light violet and brown  
403 clusters, as well as the light green and orange clusters, are more clearly separated under NRFL. In  
404 particular, the small cluster of points marked in dashed pink circle is far more separated in NRFL  
405 than other methods, indicating that NRFL enables the model to separate points belonging to different  
406 classes. Both this and the computer vision experiments establish the fact that loss functions derived  
407 from our framework improve classification performance. Next, we move on to a more challenging  
408 task, which is the information extraction task in NLP.

Loss Type	LLaMa			Qwen		
	0%	20%	50%	0%	20%	50%
CE	84.62	82.48 (1.81)	80.77 (5.44)	33.33	30.77(1.81)	26.92(5.44)
MAE	84.62	79.49 (10.88)	79.49 (7.26)	<b>79.49</b>	<b>79.49(3.63)</b>	<b>79.49(3.63)</b>
RLL	82.05	78.20 (5.44)	78.20(9.06)	76.92	75.64(1.81)	74.36(7.25)
NFL	51.28	51.28 (0.0)	46.15 (9.07)	38.46	34.62(5.44)	28.21(5.44)
GCE	21.8	20.7 (1.21)	20.7 (2.01)	15.3	13.5 (1.2)	12.8 (1.5)
APL	17.2	13.8 (1.32)	10.3 (2.14)	11.2	10.1 (1.4)	9.6 (1.4))
NRFL	<b>92.31</b>	<b>92.31 (7.25)</b>	<b>84.62 (1.81)</b>	71.79	69.23(3.63)	70.51(1.81)
WRLL	79.48	76.92 (0.0)	61.54 (0.0)	64.10	62.67(1.63)	60.26(5.44)

420 Table 4: Accuracy after LLaMa and Qwen are trained on the JSON dataset

421 **Information Extraction Task (Synthetic JSON Dataset):** The information extraction task evaluates  
422 a model’s natural language understanding capabilities. The LLM must understand a given  
423 passage and extract specific entities, such as project names, company names, and person names,  
424 which are to be returned as a JavaScript Object Notation (JSON) object. We constructed a synthetic  
425 dataset following the methodology described by Shadi Copty<sup>1</sup>. The dataset comprises 144 samples,  
426 split into training, validation, and test sets using an 80:10:10 ratio. Table 4 reports the accuracy of  
427 LLaMA and Qwen trained on the JSON dataset using various loss functions. For LLaMA, NRFL  
428 outperforms the other methods, while for Qwen, MAE and WRLL achieve higher scores. The better  
429 performance of MAE in this case is likely due to the small dataset size, which prevents underfitting  
430 and allows MAE to perform well. Figure 2b displays the convergence trajectories of models trained  
431

<sup>1</sup><https://huggingface.co/shadicopty/llama3.2-entity>

432 with different loss functions on the JSON dataset with 20% noise. NRFL exhibits stable and efficient  
 433 convergence, consistent with our observations in the computer vision experiments (Figure 2a). With  
 434 these observations, we proceed to the next challenging task which is the translation task.  
 435

Loss Type	LLaMa			Qwen		
	0%	20%	50%	0%	20%	50%
CE	51.26	51.63 (0.14)	50.71(0.33)	39.72	32.96 (2.12)	30.16 (1.12)
MAE	<b>60.37</b>	<b>60.32 (0.39)</b>	<b>60.80(0.26)</b>	<b>62.03</b>	<b>61.88 (0.02)</b>	<b>60.04 (0.11)</b>
RLL	57.78	57.78 (0.83)	58.56(0.71)	60.40	59.27 (0.10)	58.76 (0.08)
NFL	41.96	41.51 (0.60)	42.01(1.10)	34.36	34.71 (0.82)	33.38 (0.23)
NRFL	<b>58.64</b>	<b>58.75 (0.77)</b>	<b>58.27(0.61)</b>	50.37	60.02 (0.53)	59.22 (0.10)
WRLL	51.42	56.35 (7.06)	49.80(2.78)	61.72	61.77 (0.11)	<b>61.97 (0.47)</b>

Table 5: Logical equivalence score of LLaMa and Qwen trained on MALLS dataset (300 instances)

448 **Translation Task (MALLS dataset)** The main objective of this task is to convert a natural language  
 449 sentence into its corresponding first-order logic (FOL) expression. Performance on this task depends  
 450 on the model’s natural language understanding, as it has to first understand the input text and then  
 451 represent it accurately in FOL form. We use the MALLS dataset Yang et al. (2024) et al. and  
 452 introduce noise following the methodology described in their work. Following the original study,  
 453 we report the logical equivalence score, which measures the overlap between the predicted and  
 454 ground-truth FOL expressions. Table 5 presents these results. For LLaMA, NRFL performs best,  
 455 while for Qwen, WRLL ranks just after MAE. The better performance of MAE is likely due to the  
 456 small dataset size, as only 300 instances are considered, limiting underfitting. These observations  
 457 are consistent with those seen on the JSON dataset. Next we move on to a reasoning task.  
 458

Loss Type	LLaMa			LLaMa			
	0%	20%	50%	0%	20%	50%	
CE	<b>49.2</b>	48.8	48.8	CE	38.51	38.82	38.66
MAE	<b>49.1</b>	48.7	48.7	MAE	<b>40.25</b>	<b>40.1</b>	<b>40.1</b>
RLL	49.0	48.5	<b>49.1</b>	RLL	<b>41.09</b>	38.51	37.3
NFL	48.9	<b>49.2</b>	48.9	NFL	36.69	39.2	37.75
NRFL	48.5	<b>49.0</b>	48.7	NRFL	39.57	<b>40.48</b>	<b>40.25</b>
WRLL	<b>49.1</b>	<b>49.2</b>	<b>49.3</b>	WRLL	38.28	39.27	38.36

(a) OpenBookQA dataset (Accuracy $\pm 1.6$ )(b) GSM8k Dataset (Accuracy $\pm 1.3$ )

Table 6: Accuracy of LLaMa trained on different datasets on different loss functions

471 **Reasoning Task (GSM8k dataset):** Reasoning is a challenging task for LLMs, as it requires cognitive  
 472 abilities typically present in living beings such as humans. For this task, we use the GSM8k  
 473 dataset Cobbe et al. (2021), where the model has to solve a math problem by first providing the  
 474 reasoning steps and then the final numerical answer in a specified format. Note that we introduce noise  
 475 only to the final answer by randomly flipping its digits, leaving the reasoning steps intact. While  
 476 NRFL generally outperforms other loss functions, the performance gap is smaller in this case, likely  
 477 due to the presence of noise only in the final answer.

478 **Question Answering (QnA) Task (Openbook dataset):** Question answering requires an LLM  
 479 to combine natural language understanding with reasoning. The OpenBookQA dataset (Mihaylov  
 480 et al., 2018) contains questions from various domains ranging from Science, Technology, Engineering  
 481 and Mathematics (STEM) to general knowledge. Thus, the LLM needs to rely on its prior  
 482 knowledge, use it to understand the question and then generate the correct answer. Models are  
 483 trained with early stopping after 10 epochs, and the resulting accuracy scores are reported in Table  
 484 6a. As observed, NRFL and WRLL perform well across most cases. We conjecture that training  
 485 for additional epochs could further increase the performance differences among the methods. We  
 even test on a more challenging problem, which is the automatic short answer grading problem,  
 whose results have been added in Appendix B.1.

486 

## 6 CONCLUSION

488 Our proposed framework for noise-robust loss functions offers a flexible and theoretically sound  
 489 approach that improves model performance in noisy label settings. By enabling the design of  
 490 application-specific losses through monotonic functions and label normalization, this method ad-  
 491 vances the state of the art in noise robustness, as validated by strong empirical results across diverse  
 492 tasks.

493 

## REFERENCES

494 Mélanie Bernhardt, Daniel C Castro, Ryutaro Tanno, Anton Schwaighofer, Kerem C Tezcan, Miguel  
 495 Monteiro, Shruthi Bannur, Matthew P Lungren, Aditya Nori, Ben Glocker, et al. Active label  
 496 cleaning for improved dataset quality under resource constraints. *Nature communications*, 13(1):  
 497 1161, 2022.

498 Tadeusz Caliński and Jerzy Harabasz. A dendrite method for cluster analysis. *Communications in  
 499 Statistics*, 3(1):1–27, 1974. doi: 10.1080/03610927408827101.

500 YW Chen et al. On robustness of neural architecture search under label noise. *arXiv preprint  
 501 arXiv:2002.00115*, 2020. URL <https://www.ncbi.nlm.nih.gov/pmc/articles/PMC7931895/>.

502 Karl Cobbe, Vineet Kosaraju, Mohammad Bavarian, Mark Chen, Heewoo Jun, Lukasz Kaiser,  
 503 Matthias Plappert, Jerry Tworek, Jacob Hilton, Reiichiro Nakano, Christopher Hesse, and John  
 504 Schulman. Training verifiers to solve math word problems. *arXiv preprint arXiv:2110.14168*,  
 505 2021.

506 Aritra Ghosh, Himanshu Kumar, and P S Sastry. Robust loss functions under label noise for deep  
 507 neural networks. In *Proceedings of the AAAI Conference on Artificial Intelligence*, volume 31.  
 508 AAAI, 2017.

509 Kaiming He, Xiangyu Zhang, Shaoqing Ren, and Jian Sun. Deep residual learning for image recog-  
 510 nition. In *Proceedings of the IEEE Conference on Computer Vision and Pattern Recognition  
 511 (CVPR)*, pp. 770–778, 2016.

512 Ishan Jindal, Daniel Pressel, Brian Lester, and Matthew Nokleby. An effective label noise model for  
 513 dnn text classification. In *Proceedings of the 2019 Conference of the North American Chapter of  
 514 the Association for Computational Linguistics: Human Language Technologies*, pp. 3246–3256,  
 515 2019. URL <https://aclanthology.org/N19-1328/>.

516 Alex Krizhevsky. Learning multiple layers of features from tiny images. Technical Report TR-2009,  
 517 University of Toronto, 2009. CIFAR-10 and CIFAR-100 dataset introduction.

518 Ken Lang. Newsweeder: Learning to filter netnews. In *Proceedings of the Twelfth International  
 519 Conference on Machine Learning*, pp. 331–339, 1995.

520 Yann LeCun, Léon Bottou, Yoshua Bengio, and Patrick Haffner. Gradient-based learning applied to  
 521 document recognition. *Proceedings of the IEEE*, 86(11):2278–2324, 1998.

522 Jingling Li, Mozhi Zhang, Keyulu Xu, John P. Dickerson, and Jimmy Ba. How does a neural  
 523 network’s architecture impact its robustness to noisy labels? *arXiv preprint arXiv:2012.12896*,  
 524 2020. URL <https://arxiv.org/abs/2012.12896>.

525 Xingjun Ma, Hanxun Huang, Yisen Wang, Simone Romano Sarah Erfani, and James Bailey. Nor-  
 526 malized loss functions for deep learning with noisy labels. In *Proceedings of the 37th Interna-  
 527 tional Conference on Machine Learning*, ICML’20. JMLR.org, 2020a.

528 Xingjun Ma, Hanxun Huang, Yisen Wang, Simone Romano, Sarah Erfani, and James Bailey. Nor-  
 529 malized loss functions for deep learning with noisy labels. In Hal Daumé III and Aarti Singh  
 530 (eds.), *Proceedings of the 37th International Conference on Machine Learning*, volume 119 of  
 531 *Proceedings of Machine Learning Research*, pp. 6543–6553. PMLR, 13–18 Jul 2020b. URL  
 532 <https://proceedings.mlr.press/v119/ma20c.html>.

540 Meta AI. Llama 3.2: Revolutionizing edge ai and vision with open, customizable models. Meta AI  
 541 Blog, 2024. Announcement of LLaMA 3.2 models. Accessed 2025-09-03.  
 542

543 Todor Mihaylov, Peter Clark, Tushar Khot, and Ashish Sabharwal. Can a suit of armor con-  
 544 duct electricity? a new dataset for open book question answering. In *Proceedings of the 2018*  
 545 *Conference on Empirical Methods in Natural Language Processing (EMNLP)*, 2018. URL  
 546 <https://arxiv.org/abs/1809.02789>. arXiv preprint arXiv:1809.02789.

547 Alexandre Lemire Paquin, Brahim Chaib-draa, and Philippe Giguère. Symmetrization of loss func-  
 548 tions for robust training of neural networks in the presence of noisy labels and the multi-class un-  
 549 hinged loss function, 2024. URL <https://openreview.net/forum?id=MY7gMVioiX>.  
 550

551 Hamid Rezatofighi, Nathan Tsoi, JunYoung Gwak, Amir Sadeghian, Ian Reid, and Silvio Savarese.  
 552 Generalized intersection over union: A metric and a loss for bounding box regression. In *Pro-  
 553 ceedings of the IEEE/CVF Conference on Computer Vision and Pattern Recognition (CVPR)*, pp.  
 554 658–666, 2019.

555 Peter J. Rousseeuw. Silhouettes: a graphical aid to the interpretation and validation of clus-  
 556 ter analysis. *Journal of Computational and Applied Mathematics*, 20(1):53–65, 1987. doi:  
 557 [10.1016/0377-0427\(87\)90125-7](https://doi.org/10.1016/0377-0427(87)90125-7).

559 Aryan Sajith, Rajesh Gupta, Anjali Kumar, and Hyunwoo Lee. Is training data quality or  
 560 quantity more impactful to small and medium-scale large language models? *arXiv preprint  
 561 arXiv:2411.15821*, 2024. URL <https://arxiv.org/abs/2411.15821>.

562 Christian Szegedy, Wei Liu, Yangqing Jia, Pierre Sermanet, Scott E. Reed, Dragomir Anguelov,  
 563 Dumitru Erhan, Vincent Vanhoucke, and Andrew Rabinovich. Going deeper with convolutions. In  
 564 *Proceedings of the 2015 IEEE Conference on Computer Vision and Pattern Recognition (CVPR)*,  
 565 2015. arXiv:1409.4842.

566 Qwen Team. Qwen2.5-0.5b-instruct, 2025. URL <https://huggingface.co/Qwen/Qwen2.5-0.5B-Instruct>. Accessed: 2025-09-25.

569 Rahul Vashisht, P. Krishna Kumar, Harsha Vardhan Govind, and Harish G. Ramaswamy. Impact of  
 570 label noise on learning complex features. *arXiv preprint arXiv:2411.04569*, 2024. URL <https://arxiv.org/abs/2411.04569>.

573 Ashish Vaswani, Noam Shazeer, Niki Parmar, Jakob Uszkoreit, Llion Jones, Aidan N Gomez,  
 574 Łukasz Kaiser, and Illia Polosukhin. Attention is all you need. *Advances in neural informa-  
 575 tion processing systems*, 30, 2017.

576 Pengxiang Wu, Songzhu Zheng, Mayank Goswami, Dimitris Metaxas, and Chao Chen. A topolog-  
 577 ical filter for learning with label noise. *Advances in neural information processing systems*, 33:  
 578 21382–21393, 2020.

580 Han Xiao, Kashif Rasul, and Roland Vollgraf. Fashion-mnist: a novel image dataset for benchmark-  
 581 ing machine learning algorithms. *arXiv preprint arXiv:1708.07747*, 2017.

582 Yuan Yang, Siheng Xiong, Ali Payani, Ehsan Shareghi, and Faramarz Fekri. Harnessing the power  
 583 of large language models for natural language to first-order logic translation. In *Proceedings of the*  
 584 *62nd Annual Meeting of the Association for Computational Linguistics (Volume 1: Long Papers)*,  
 585 pp. 6942–6959, Bangkok, Thailand, aug 2024. Association for Computational Linguistics. doi:  
 586 [10.18653/v1/2024.acl-long.375](https://doi.org/10.18653/v1/2024.acl-long.375).

588

589 **APPENDIX**  
 590

591 **A EXPERIMENTAL SETUP**  
 592

593 The hyperparameters used for each and every experiment is mentioned in each subsection below.

594 A.1 OBJECT CLASSIFICATION TASK  
595596 A learning rate of  $10^{-4}$  was used for all loss functions, except for NRFL and WRLL, where a higher  
597 learning rate of  $10^{-3}$  was adopted, with a batch size of 2048. For NRFL, the gradient update is  
598 computed as

599 
$$600 w' = w - \eta \frac{\delta L}{\delta w},$$
  
601

602 where update term includes a factor of  $\eta \cdot \gamma$ . Since the optimal  $\gamma$  was determined empirically between  
603 0.01 and 2.0 as 0.01, the effective learning rate becomes  $10^{-5}$ . Consequently, we maintain a higher  
604 learning rate for NRFL to compensate. To simulate label noise, we randomly flip x% of the labels  
605 in the dataset and generate two instances each for 30% and 60% noisy datasets.

606

607 A.2 NLP-BASED CLASSIFICATION TASK (NEWS20 DATASET)  
608609 For this set of experiments, we train LLaMA for 100 epochs using a learning rate of  $10^{-5}$  and a  
610 batch size of 40, with  $\gamma = 0.01$ . Dimensionality reduction on the embeddings generated by the  
611 model is performed using UMAP, with the following parameters:612 

- 613 • n\_components: 2
- 614 • n\_neighbors: 15
- 615 • min\_dist: 1.0
- 616 • metric: 'euclidean'
- 617 • random\_state: 21

  
618619 To simulate label noise, we randomly flip x% of the labels in the dataset and generate a single  
620 instance of a 20% noisy dataset.

621

622 A.3 INFORMATION EXTRACTION TASK (JSON DATASET)  
623624 For these experiments, the models were trained for 100 epochs with a learning rate of  $10^{-5}$  for all  
625 methods, except for NRFL and WRLL, which used a learning rate of  $10^{-4}$  for the reasons described  
626 earlier. A batch size of 40 was used, and  $\gamma$  for NRFL was set to 0.01.627 To simulate label noise, 20% and 50% of the samples in the training set were corrupted by randomly  
628 flipping entity names within the target JSON objects. For each noise level, two instances were  
629 created, and results were averaged across both.

630

631 A.4 TRANSLATION TASK (MALLS DATASET)  
632633 For this set of experiments, the models were trained for 100 epochs with a batch size of 40 and a  
634 learning rate of  $10^{-5}$ . Note that only the first 300 instances of the MALLS dataset were used.635 To introduce noise, we follow the methodology of Yang et al. (2024) et al.. For each data instance  
636 where noise is applied, only one of the perturbations listed in Table 7 is selected. Similarly, two  
637 instances of each noise level were created, and the reported results correspond to the mean and  
638 standard deviation across both instances.

639

640 A.5 REASONING AND QNA TASK  
641642 For both of these experiments, we use a learning rate of  $10^{-5}$ , train for 10 epochs, and set a batch  
643 size of 40. Noise is added to 20% and 50% of the datapoints in both datasets. For GSM8k, noise  
644 is applied only to the final answer, which is a number, by randomly flipping its digits. For Open-  
645 BookQA, the correct answer is randomly flipped to an incorrect one.

648 649 650 651 652 653 654 655 656 657 658 659 660 661 662 663 664 665 666 667 668 669 670 671 672 673 674 675 676 677 678 679 680 681 682 683 684 685 686 687 688 689 690 691 692 693 694 695 696 697 698 699 700 701	Operation Type	Subtype	Original	Perturbed
Label Change	Change Predicate	$P(A) \wedge R(B)$	$R(A) \wedge R(B)$	
	Change Term	$\forall x P(x) \wedge P(B)$	$\forall y P(x) \wedge P(B)$	
	Change Operator	$\forall x P(x) \wedge P(B)$	$\forall x P(x) \wedge P(x)$	
Insert	Insert Term	$\forall x P(x) \wedge P(B)$	$\forall x \exists y P(x) \wedge P(B)$	
	Insert Negation	$\forall x P(x) \wedge P(B)$	$\forall x P(x) \wedge P(x, B)$	
	Insert Formula	$P(A) \wedge P(B) \wedge P(C)$	$P(A) \wedge \neg(P(B) \wedge P(C))$	
Delete	Delete Term	$\forall x \forall y P(x) \wedge R(x, y)$	$\forall y P(x) \wedge R(x, y)$	
	Delete Negation	$\forall x \forall y P(x) \wedge R(x, y)$	$\forall x \forall y P(x) \wedge R(y)$	
	Delete Formula	$\neg(P(A) \wedge P(B))$	$P(A) \wedge P(B)$	
		$P(A) \wedge P(B) \wedge P(C)$	$P(A) \wedge P(C)$	

Table 7: The list of all atomic perturbations.

Loss Type	UQ			UA		
	0%	20%	50%	0%	20%	50%
CE	19.18	24.49	15.45	17.12	21.69	14.93
MAE	22.13	14.61	18.64	14.04	16.53	16.76
RLL	37.26	26.21	22.25	30.61	22.93	21.67
NFL	20.17	7.58	5.31	14.25	5.36	6.23
NRFL	41.56	16.32	19.62	47.73	20.45	18.93
WRLL	9.42	8.97	9.5	6.25	5.67	5.69

Table 8: Accuracy of LLaMa trained on ASAG dataset

## B EXTENDED EXPERIMENTAL EVALUATION

### B.1 AUTOMATIC SHORT ANSWER GRADING TASK

Finally, we consider an Automatic Short Answer Grading task, given a question and a reference answer, and the LLM must generate a score for a student’s response. This task requires both natural language understanding and comparative reasoning capabilities between the two answers. Results indicate that NRFL outperforms other methods in most cases. In contrast, WRLL performs poorly, as it is better suited for classification tasks with label noise. Given the reasoning-intensive nature of this task, NRFL is more effective than WRLL. We conjecture that noise-robust reinforcement learning techniques may be better suited for such tasks than standard supervised fine-tuning using noise robust loss functions.

### B.2 EVALUATION OF RESNET18 ON CIFAR-100 DATASET

Loss Function	0%	30%	60%
CE	52.87	51.43	41.60
RLL	41.53	41.02	26.44
NFL	12.43	9.01	6.10
GCE	51.92	53.50	39.38
NRFL	55.98	49.01	35.29
WRLL	54.45	52.29	42.09

Table 9: Accuracy of ResNet-18 after training on CIFAR-100 dataset

702 ResNet-18 has been trained on the CIFAR-100 dataset for 400 epochs, along with a learning rate  
703 of 0.1 for all loss functions. It can again be observed from Table 9 that our methods outperform  
704 others, including recent loss functions like GCE. We attribute this improvement to the model’s ability  
705 to learn more discriminative decision boundaries, consistent with the patterns observed in earlier  
706 experiments (as in Figure 1).

707

708

709

710

711

712

713

714

715

716

717

718

719

720

721

722

723

724

725

726

727

728

729

730

731

732

733

734

735

736

737

738

739

740

741

742

743

744

745

746

747

748

749

750

751

752

753

754

755